Cross-Structure Loads of a Simple SWATH Vessel

Thomas Mathai
The Glosten Associates, Inc.
Seattle, WA, USA

ABSTRACT

Wave-induced cross-structure loads are presented for a SWATH (Small Waterplane Area Twin Hull) vessel whose hull is made up of simple geometrical shapes. The hydrodynamic problem is solved using the higher-order boundary element method and the generalized modes approach available in the radiation-diffraction program WAMIT (Lee and Newman, 2001). The difference between cross-structure loads computed in earth-fixed coordinates and the same loads computed in body-fixed coordinates is illustrated. In the absence of any damping from viscous effects and separation, the computed free surface elevation in the gap between the hulls exhibits large sloshing at resonant frequencies. The effect of sloshing resonance on the computed loads is shown. A technique proposed by Newman (2004) to simulate the additional damping and thereby obtain more realistic predictions of free surface elevations and cross-structure loads is demonstrated.

KEY WORDS: Radiation; diffraction; SWATH; generalized modes; sloshing; gap resonance.

INTRODUCTION

In modern ship design practice, theoretically determined loads are often used along with finite element methods to assess the global and local ship structure response. For example, the *dynamic loading approach* (DLA) established by the American Bureau of Shipping (ABS) provides a 'design by iterative analysis' framework to complement the traditional semi-empirical, rule-based design (Liu, Spencer, Itoh, Kawachi and Shigematsu, 1992). For SWATH (Small Waterplane Area Twin Hull) vessels, the ABS guide (1999) defines the load cases that typically need to be considered. These, shown schematically in Fig. 1, all stem from the differential loading on the two hulls.

It is possible to compute these differential loads by solving the hydrodynamic problem for the six rigid modes of the SWATH vessel in the usual manner, and then integrating the resulting pressure over the submerged surface of each hull separately to get individual hull forces. However, integration of panel pressures in a post-processor requires the handling of large data files and is cumbersome. Use of local panel pressures also precludes the application of Haskind relations, which are capable of providing solutions for multiple wave headings with minimum computational effort. These difficulties can be circumvented by adopting the generalized mode approach outlined by Newman (1994). Application of this technique to the particular case of a SWATH vessel has been illustrated by Mathai (2000). In the present paper, the same technique is applied to a SWATH vessel whose geometry is defined by simple shapes: a pair of tubular lower hulls with hemispherical ends, a pair of box struts and a box cross structure. The simplicity of the geometry permits the definition of the wetted surface through an analytical representation of higher-order boundary elements. A complete set of cross-structure loads is presented.

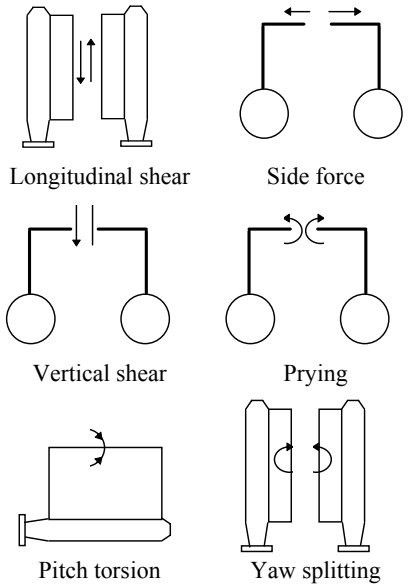

Fig 1. Differential loads for a SWATH vessel (ABS, 1999)

The difference between cross-structure loads computed in earth-fixed coordinates and body-fixed coordinates is examined. Sharp peaks are found in the load response amplitude operator (RAO) curves at frequencies corresponding to the natural frequencies of vessel response as well as frequencies of sloshing resonance in the gap between the struts. These peaks are exaggerated due to lack of viscous damping and

separation in the calculations. In practical applications, external damping could be added to the resonant vessel response modes as long as there is some basis for estimating the level of damping to be added. This will mitigate the unrealistically large peaks at the natural frequencies of vessel response. Likewise, to mitigate the peaks at the frequencies of sloshing resonance, Newman's (2004) technique of adding damping to the sloshing modes is helpful. The application of this technique to sloshing in the gap between the struts is illustrated in this paper.

THEORETICAL FORMULATION

Equations of Motion

In the computation of wave-induced vessel motions, it is convenient to refer to an earth-fixed right-handed Cartesian coordinate system with the origin coinciding with the still water level, the x axis pointing forward, y axis pointing to port and the z axis pointing vertically up. The motions of a rigid body can be described by defining three translatory modes parallel to the axes (surge, sway and heave) and three rotatory modes about the axes (roll, pitch and yaw). These modes are denoted by the indices j = 1, 2, . . 6. Each mode may be represented by a vector shape function $\mathbf{S}j(\mathbf{x})$ with Cartesian components (U_j, V_j, W_j). Throughout the paper, boldface is used to denote vector quantities. The shape function $\mathbf{S}j(\mathbf{x})$ gives the excursion of a point $\mathbf{x}$ on the body when the body is displaced by one unit in the j^{th} mode. Thus, for rigid-body translations (j = 1, 2, 3), the shape function $\mathbf{S}j$ is a unit vector in the corresponding direction. For rigid-body rotations (j = 4, 5, 6), $\mathbf{S}j(\mathbf{x}) = \mathbf{S}_{j-3} \times \mathbf{x}$ where $\times$ denotes cross multiplication.

The complex amplitudes of vessel motions in a unit-amplitude monochromatic wave, ξ_j, j = 1, 2, . . 6, are determined by solving the linear system obtained by applying Newton's law:

$$\sum_{j=1}^{6} \{-\omega^2 [\mu_{ij}(\omega)+M_{ij}] + i\omega\lambda_{ij}(\omega) + C_{ij}\} \xi_j(\omega;\theta) = \chi_i(\omega;\theta) \qquad i = 1, 2, . . 6 \tag{1}$$

Here, χ_i is the complex amplitude of wave excitation force in the i^{th} mode, μ_{ij} is the coupling added mass between the i^{th} and j^{th} modes, M_{ij} is the structural mass, λ_{ij} is the damping coefficient and C_{ij} is the stiffness (including hydrostatic and gravitational restoring). Also, ω denotes angular frequency, θ is the angle of wave incidence measured anti-clockwise (when looking in the negative z direction) from the positive x axis and i denotes $\sqrt{-1}$. The time factor $\exp(i\omega t)$ has been factored out from Eq. 1. Complex algebra is adopted with the understanding that the temporal variation of a quantity is to be eventually obtained by multiplying the complex amplitude by the time factor and then taking the real part.

The elements in the structural mass matrix are given by the following equation (see Eq. 140, page 149 of Newman, 1986):

$$M_{ij} = \int_V \rho_S(\mathbf{x})\, \mathbf{S}_i(\mathbf{x}) \bullet \mathbf{S}_j(\mathbf{x})\, dV \tag{2}$$

where ρ_S is the density of the structure, $\mathbf{S}_i$ is the shape function for the i^{th} mode, $\bullet$ denotes dot product, and the integration is over V, the entire volume of the structure. The symmetry of the mass matrix is evident from Eq. 2. The following equation gives the hydrostatic restoring coefficients in earth-fixed coordinates (see Eq. 2.17 of Newman, 1994):

$$c_{ij} = \rho g \int_{S_0} [W_i(\mathbf{x}) + z D_i][\mathbf{S}_j(\mathbf{x}) \bullet \mathbf{n}]\, dS \tag{3}$$

where ρ is the fluid density, g is gravitational acceleration, $\mathbf{n}$ is the unit vector normal to the body boundary pointing into the body and S_0 denotes the mean body wetted surface. D_i is the divergence of $\mathbf{S}_i$, which vanishes for the type of mode shapes treated here. The elements in the stiffness matrix are obtained by adding gravitational restoring terms to the hydrostatic restoring terms determined from Eq. 3. The form of Eq. 3 indicates that the stiffness matrix is not symmetric in general. In fact, it can be shown that the stiffness matrix in a body-fixed coordinate system (which coincides with the earth-fixed system when the body is at rest) is the transpose of the stiffness matrix in the earth-fixed system. This distinction between earth-fixed coordinates and body-fixed coordinates is important and must be retained in the definition of the stiffness. The stiffness matrix used in the solution of the equations of motion (Eq. 1) must be defined in earth-fixed coordinates. On the other hand, structural loads are best described in body-fixed coordinates for input to structural calculations. The calculation of structural loads, once the motions are known, must therefore employ a stiffness matrix defined in body-fixed coordinates.

The hydrodynamic parameters χ_i, μ_{ij} and λ_{ij} in Eq. 1 are frequency-dependent and their determination constitutes the bulk of the computational effort in fluid-structure interaction problems. Typically a radiation-diffraction panel program is used for this purpose.

SWATH Vessel

A schematic of a SWATH vessel made up of simple shapes is shown in Fig. 2. The lower hulls are submerged, and are tubular with length L and radius r. They are attached to hemispherical ends. Box-shaped struts, with length L and thickness t, connect the lower hulls to the cross structure. The draft of the vessel is T and the hull spacing centerline to centerline is w. The cross structure is a box with length L. The bottom of this box (wet deck) is z_w distance above still water level (SWL). The top of this box (main deck) is z_m distance above SWL.

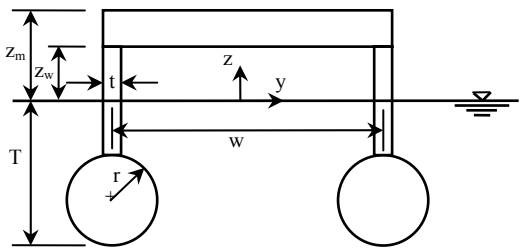

Fig. 2. Cross-sectional sketch of SWATH vessel

The vessel is symmetric about the vertical center plane y = 0. The conventional rigid-body modes are denoted by the indices j = 1, 2, . . 6 with the shape functions described at the beginning of the previous subsection. The notation is further extended to cover six additional generalized modes, j = 7, 8, . . 12, in which the port hull and the starboard hull move in opposite directions. Their shape functions are prescribed as:

$$\mathbf{S}_j = \begin{cases} \mathbf{S}_{j-6} & y > 0 \\ -\mathbf{S}_{j-6} & y < 0 \end{cases} \qquad j = 7, 8, . . 12 \tag{4}$$

It is to be noted that the mode shapes of Eq. 4 preserve the computational advantage offered by the geometric symmetry of the SWATH vessel since they are either symmetric or anti-symmetric about the y = 0 plane.

The exciting forces and hydrodynamic coefficients for the combined set of free (1 to 6) and fixed (7 to 12) modes are first computed using a

radiation-diffraction panel program. The motion amplitudes, ξ_j, j = 1, 2, . . 6, are then determined by solving the six coupled equations of motion for the free modes alone (Eq. 1). Once the vessel motions are determined, the loads in the fixed modes are evaluated as follows:

$$F_i(\omega;\theta) = \chi_i(\omega;\theta) + \sum_{j=1}^{6} \{\omega^2 [\mu_{ij}(\omega) + M_{ij}] - i\omega\lambda_{ij}(\omega) - C'_{ij}\} \xi_j(\omega;\theta) \quad (5)$$
$$i = 7, 8, . . 12$$

where F_i is the complex amplitude of the load in the i^{th} mode for an incident wave of frequency ω and heading θ, and C'_{ij} is the coupling stiffness in vessel-fixed coordinates.

To determine the differential loads in Fig. 1, the generalized forces from Eq. 5 need to be divided by two and transferred to a new coordinate system with the origin located at the level of the cross structure instead of the still water level. The equations for the differential loads are given below.

$$f_i = \frac{F_i}{2} \qquad i = 7, 8, 9, 12 \quad (6)$$

$$f_{10} = \frac{F_{10} + z_d F_8}{2} \quad (7)$$

$$f_{11} = \frac{F_{11} - z_d F_7}{2} \quad (8)$$

In Eqs. 7 and 8, z_d is the height of cross structure above still water level, taken as:

$$z_d = \frac{z_w + z_m}{2} \quad (9)$$

Sloshing Modes

In the absence of any damping from viscous effects and separation, the computed free surface elevation in the gap between the hulls will exhibit large sloshing at resonant frequencies. To mitigate this, Newman's (2004) technique of adding external damping to the sloshing modes can be applied. For this, a flexible lid is placed on the free surface in the gap. This lid is assumed to be mass-less and is allowed to respond in wave-like vertical motion. The vertical motion is represented by an appropriate set of basis functions. These are treated as additional generalized modes that have to be solved simultaneously along with the rest of the modes in the coupled equations of motion. The adequacy of the selected set of basis functions has to be first verified by computing the lid deflection without any external damping, and comparing it to the free surface elevation in the gap computed without the lid. A close match indicates that the selected set is sufficient. External damping could be then added to these modes to damp out sloshing resonance.

RESULTS

The example SWATH vessel used in the calculations has the dimensions given in Table 1.

Table 1. Dimensions of the example SWATH vessel

Length, L	106' (32.31 m)
Hull spacing, w	41.5' (12.65 m)
Lower hull radius, r	4.375' (1.33 m)
Draft, T	12' (3.66 m)
Strut thickness, t	2.83' (0.86 m)
Wet deck height (above SWL), z_w	8' (2.44 m)
Main deck height (above SWL), z_m	13' (3.96 m)
Vertical center of gravity (above SWL), z_g	6.75' (2.06 m)

This gives a total displacement of 440 long tons (447.22 tonnes). The two lower hulls together weigh 91 long tons (92.53 tonnes) and the cross structure weighs 349 long tons (354.69 tonnes). Mass is assumed to be distributed uniformly inside the lower hulls and in the cross structure. The mass of the struts is assumed to be negligible.

Figure 3 shows the higher-order boundary element model with panel subdivisions. The light gray patch on the free surface is the flexible lid introduced later for modeling sloshing modes.

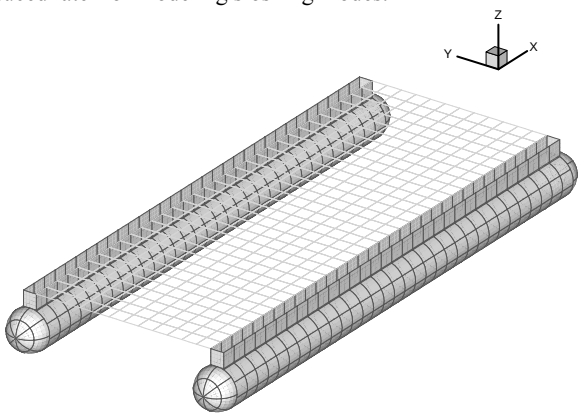

Fig. 3. Higher-order boundary element model showing panel subdivisions

The RAOs of the cross-structure loads are presented in Figs. 5a-f for 30, 60 and 90 degree wave incidence. The forces and moments have been non-dimensionalized by the fluid density ρ, gravitational acceleration g, length L, draft T and wave amplitude A. They are plotted as a function of Kw/2π where K is the wave number and w is the transverse spacing between the lower hulls. In case of pitch torsion and yaw splitting, there is a distinction between earth-fixed coordinates and vessel-fixed coordinates as discussed previously. For these modes, loads in both sets of coordinates have been presented side by side in Figs. 5e-f. Although the difference appears to be relatively small in this particular example, it is important to note that, in general, loads have to be in vessel-fixed coordinates for input to structural calculations.

The peak in vertical shear when Kw/2π is 0.033, the peak in prying when it is 0.16 and the peak in vessel-fixed yaw splitting when it is 0.095 are caused by roll, heave and pitch resonance respectively. These peaks are exaggerated due to lack of viscous damping and separation in the calculations. They could be mitigated by adding external damping to roll, heave and pitch modes as long as there is some basis for estimating the level of damping to be added.

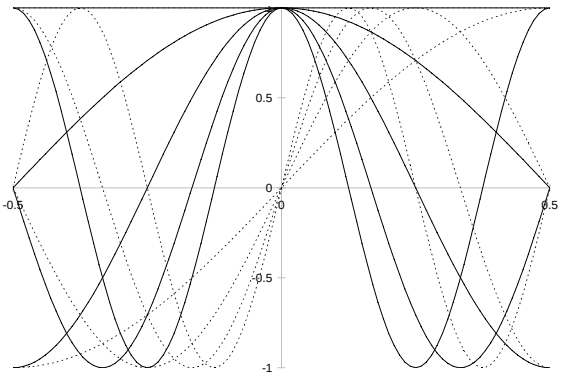

Fig. 4. Basis functions for sloshing modes; ——, cosine; ·····, sine

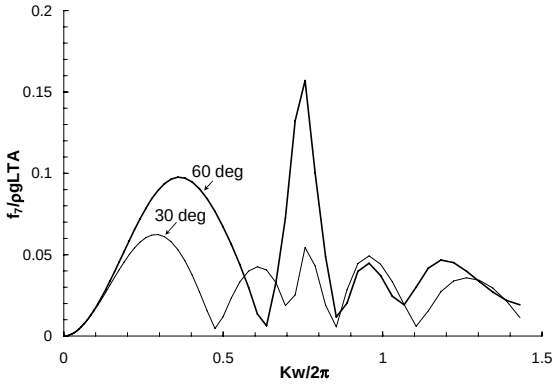

(5a) Longitudinal shear

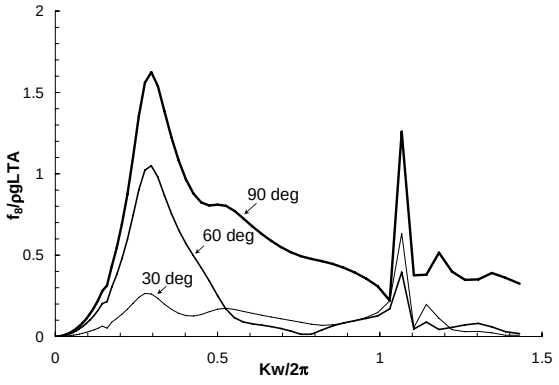

(5b) Side force

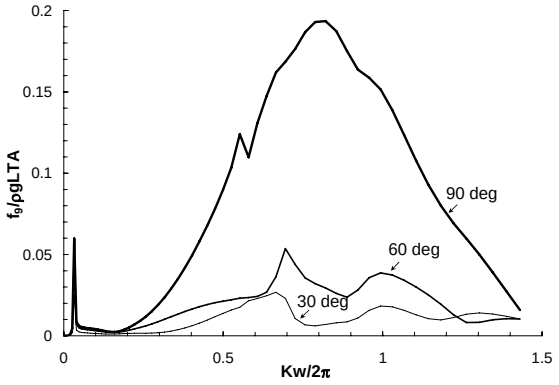

(5c) Vertical shear

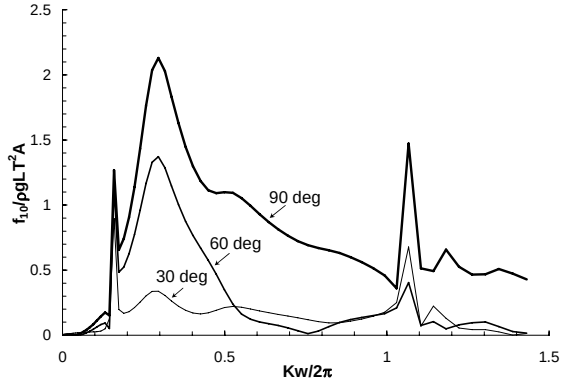

(5d) Prying

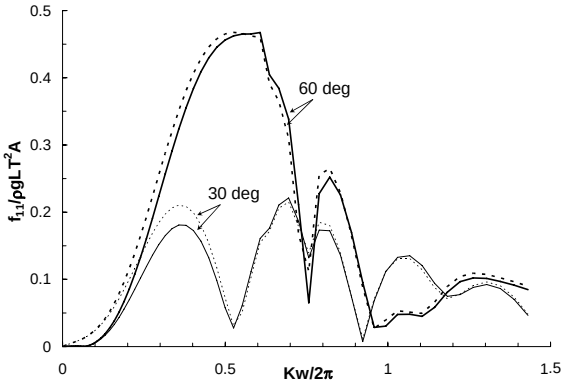

(5e) Pitch torsion

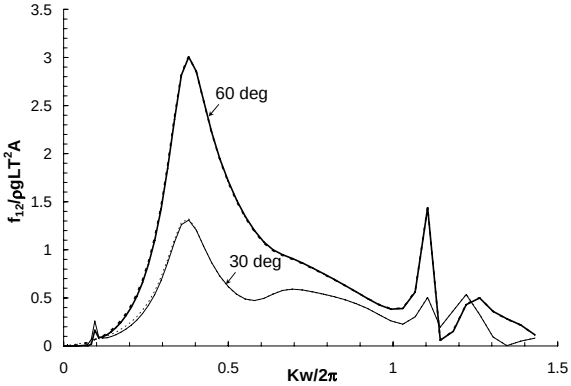

(5f) Yaw splitting

Fig. 5. Differential load RAOs for 30, 60 & 90 degree wave incidence. ——, vessel-fixed co-ordinates; ·····, earth-fixed co-ordinates

Additionally, the side force, prying and yaw splitting exhibit a peak when $Kw/2\pi$ is about 1.1. This value of $Kw/2\pi$ corresponds to a wave length which closely matches the gap between the struts. This peak is attributable to sloshing resonance in the gap. To mitigate this, a flexible lid is placed on the free surface in the gap as indicated by the light gray patch in Fig. 3. This lid is assumed to be mass-less and is allowed to respond in wave-like vertical motion. The vertical motion is described by a set of 81 generalized modes. The mode shapes are composed of the 9 trigonometric functions of Fig. 4 applied both longitudinally and transversely. The lid deflection is then computed and compared to the free surface elevation in the gap without the lid. This comparison is shown in Fig. 6 for 90 degree wave incidence and for three transverse locations. The circular symbols denote the conventional computation of the free surface elevation. The dotted line denotes the deflection of the lid. Except for slight discrepancies at a few frequencies near the high end of the frequency range, the lid deflection matches the free surface elevation fairly closely. The calculations are then repeated after adding a constant damping coefficient to all 81 sloshing modes. The solid lines in Fig. 6 show the lid deflection with two different levels of damping. As expected, resonant sloshing is progressively reduced with increasing levels of damping. Figure 7 demonstrates the effect this has on the computed cross-structure loads where a similar reduction in the peak near sloshing resonance is evident.

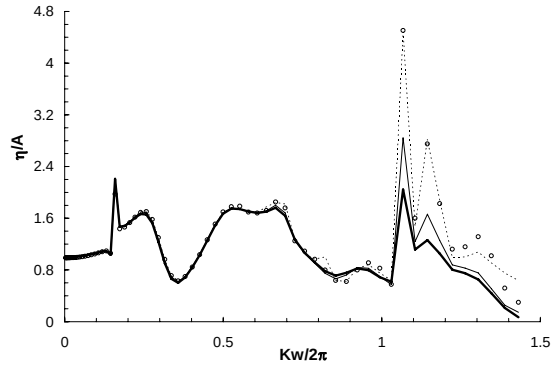

(6a) Starboard

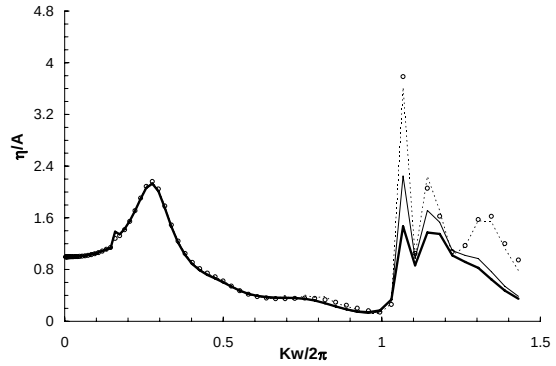

(6b) Center

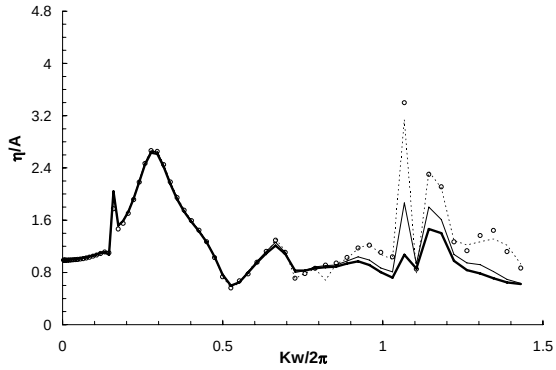

(6c) Port

Fig. 6. Wave elevation RAOs at three transverse locations mid-ship below wet deck for 90 degree wave incidence.
o, without lid; ……, sloshing damping 0; ——, sloshing damping 500; ▬▬, sloshing damping 1,000

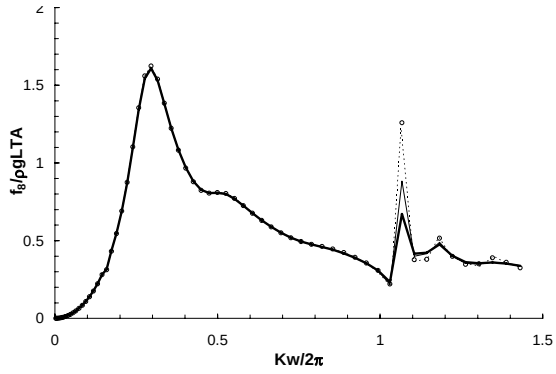

(7a) Side force

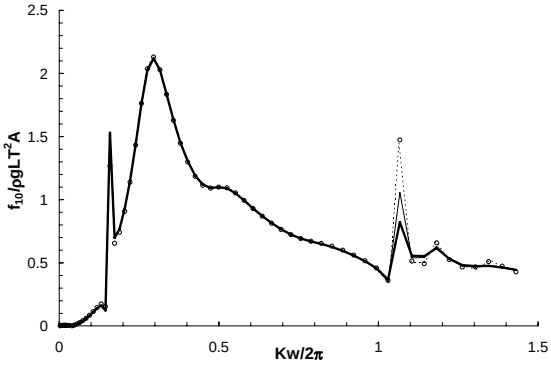

(7b) Prying

Fig. 7. Differential load RAOs for 90 degree wave incidence.
o, without lid; ……, sloshing damping 0; ——, sloshing damping 500; ▬▬, sloshing damping 1,000

CONCLUSION

Cross-structure loads are presented for a SWATH vessel whose geometry is defined by simple shapes. The difference between loads computed in earth-fixed coordinates and vessel-fixed coordinates is examined. Sharp peaks in the computed load RAOs are traced to either resonant response of the vessel in heave, roll and pitch, or sloshing resonance in the gap between the struts. Newman's technique is applied to damp the sloshing modes and obtain more realistic predictions of free surface elevations and cross-structure loads near sloshing resonance. The advantage of this method lies in being able to calibrate the potential flow model if data on actual sloshing amplitudes is available.

It is to be noted that the calculations described are all linear in wave steepness. Non-linear effects like the change in hydrostatic stiffness due to hull emergence, which is an important factor in the analysis of vessels of this type, are not addressed here.

ACKNOWLEDGEMENTS

The author is grateful to his employer for permission to write this paper. Thanks to Prof. Nick Newman and Dr. Chang-Ho Lee for help with WAMIT. Special thanks to Linda Dailey for editorial help.

REFERENCES

ABS (1999). *Guide for Building and Classing Small Water Plane Area Twin Hull (SWATH) Vessels.*

Lee, C-H, and Newman, JN (2001). "Solution of Radiation Problems with Exact Geometry," *16th International Workshop on Water Waves and Floating Bodies*, Hiroshima, Japan.

Liu, D, Spencer, J, Itoh, T, Kawachi, S, and Shigematsu, K (1992). "Dynamic Load Approach in Tanker Design," *SNAME Transactions*, Vol 100, pp 143-172.

Mathai, T (2000). "Use of Generalized Modes in Hydrodynamic Analysis of Multiple Bodies," *Proceedings of the Tenth (2000) International Offshore and Polar Engineering Conference*, Seattle, USA, pp 396-401.

Newman, JN (1986). *Marine Hydrodynamics*, The MIT Press, Cambridge.

Newman, JN (1994). "Wave Effects on Deformable Bodies," *Applied Ocean Research*, Vol 16, pp 47-59.

Newman, JN (2004). "Progress in Wave Load Computations on Offshore Structures," Invited Lecture, 23rd OMAE Conference, Vancouver, Canada, http://www.wamit.com/newman_omae04.pdf.